A Chemical Glycoproteomics Platform Reveals O-GlcNAcylation of Mitochondrial Voltage-Dependent Anion Channel 2

Krishnan K. Palaniappan,[1] Matthew J. Hangauer,[1] Timothy J. Smith,[2] Brian P. Smart,[1] Austin A. Pitcher,[1] Emily H. Cheng,[3] Carolyn R. Bertozzi,[1,4,5,*] and Michael Boyce[1,2,*]

[1]Department of Chemistry, University of California, Berkeley, Berkeley, CA 94720, USA
[2]Department of Biochemistry, Duke University School of Medicine, Durham, NC 27710, USA
[3]Human Oncology and Pathogenesis Program and Department of Pathology, Memorial Sloan-Kettering Cancer Center, New York, NY 10065, USA
[4]Department of Molecular and Cell Biology, University of California, Berkeley, Berkeley, CA, 94720, USA
[5]Howard Hughes Medical Institute, University of California, Berkeley, Berkeley, CA 94720, USA
*Correspondence: crb@berkeley.edu (C.R.B.), michael.boyce@duke.edu (M.B.)
http://dx.doi.org/10.1016/j.celrep.2013.08.048

SUMMARY

Protein modification by O-linked β-*N*-acetylglucosamine (O-GlcNAc) is a critical cell signaling modality, but identifying signal-specific O-GlcNAcylation events remains a significant experimental challenge. Here, we describe a method for visualizing and analyzing organelle- and stimulus-specific O-GlcNAcylated proteins and use it to identify the mitochondrial voltage-dependent anion channel 2 (VDAC2) as an O-GlcNAc substrate. $VDAC2^{-/-}$ cells resist the mitochondrial dysfunction and apoptosis caused by global O-GlcNAc perturbation, demonstrating a functional connection between O-GlcNAc signaling and mitochondrial physiology through VDAC2. More broadly, our method will enable the discovery of signal-specific O-GlcNAcylation events in a wide array of experimental contexts.

INTRODUCTION

Modification of intracellular proteins by O-linked β-*N*-acetylglucosamine (O-GlcNAcylation) has emerged recently as a ubiquitous cell signaling modality in a broad range of organisms, influencing such core cell biological processes as transcription, nutrient sensing, and cell-cycle progression (Hanover et al., 2010; Hart et al., 2011). Analogous to phosphorylation, O-GlcNAcylation is a dynamic, rapidly cycling posttranslational modification that modulates substrate proteins' location, function, or stability in response to physiological signals (Hanover et al., 2010; Hart et al., 2011). Accordingly, it is of great interest to identify which substrate proteins are O-GlcNAcylated in response to a given biological cue. However, this goal poses a substantial experimental challenge, in part because rare, signal-dependent changes in O-linked β-*N*-acetylglucosamine

(O-GlcNAc) are difficult to detect amidst the large number of abundant, constitutively, and multiply glycosylated "background" proteins (e.g., nucleoporins). Although chemical (Wells et al., 2002), chemoenzymatic (Khidekel et al., 2003), lectin- (Vosseller et al., 2006), and antibody- (Teo et al., 2010) based methods for identifying O-GlcNAcylated proteins have been described, these approaches all rely on affinity purification to enrich substrates and are therefore inherently biased toward abundant, unchanging "background" O-GlcNAc, at the expense of the comparatively rare, substoichiometric, signal-dependent changes in O-GlcNAc. Therefore, new, complementary methods are needed for identifying functionally relevant changes in protein O-GlcNAcylation.

We have previously described a strategy for identifying O-GlcNAcylated proteins in living mammalian cells using the unnatural azide-functionalized sugar *N*-azidoacetylgalactosamine (GalNAz) as a metabolic label (Boyce et al., 2011). Briefly, we showed that GalNAz is converted by endogenous metabolic enzymes to the nucleotide-sugar UDP-GalNAz and then epimerized to UDP-*N*-azidoacetylglucosamine (GlcNAz), the azido analog of natural UDP-GlcNAc (Boyce et al., 2011; Vocadlo et al., 2003). O-GlcNAc transferase (OGT) accepts UDP-GlcNAz as a nucleotide-sugar donor, resulting in the installation of "O-GlcNAz" on native OGT substrates (Figure 1A) (Boyce et al., 2011; Vocadlo et al., 2003). The resulting azide-functionalized ("O-GlcNAzylated") proteins can then be chemically tagged using any of several classes of azide-reactive probes (Figure 1A) (Boyce and Bertozzi, 2011; Boyce et al., 2011). Importantly, this strategy allows for selective labeling of new O-GlcNAc moieties (i.e., those formed after GalNAz is added to cells), affording time-resolution control not provided by other methods of O-GlcNAc detection. We have previously used affinity probes to purify bulk endogenous, O-GlcNAzylated proteins, revealing numerous known O-GlcNAc substrates and demonstrating that GalNAz is a faithful and robust metabolic reporter of cellular O-GlcNAc (Boyce et al., 2011). Here, we build upon our GalNAz metabolic-labeling strategy to create a proteomics platform for
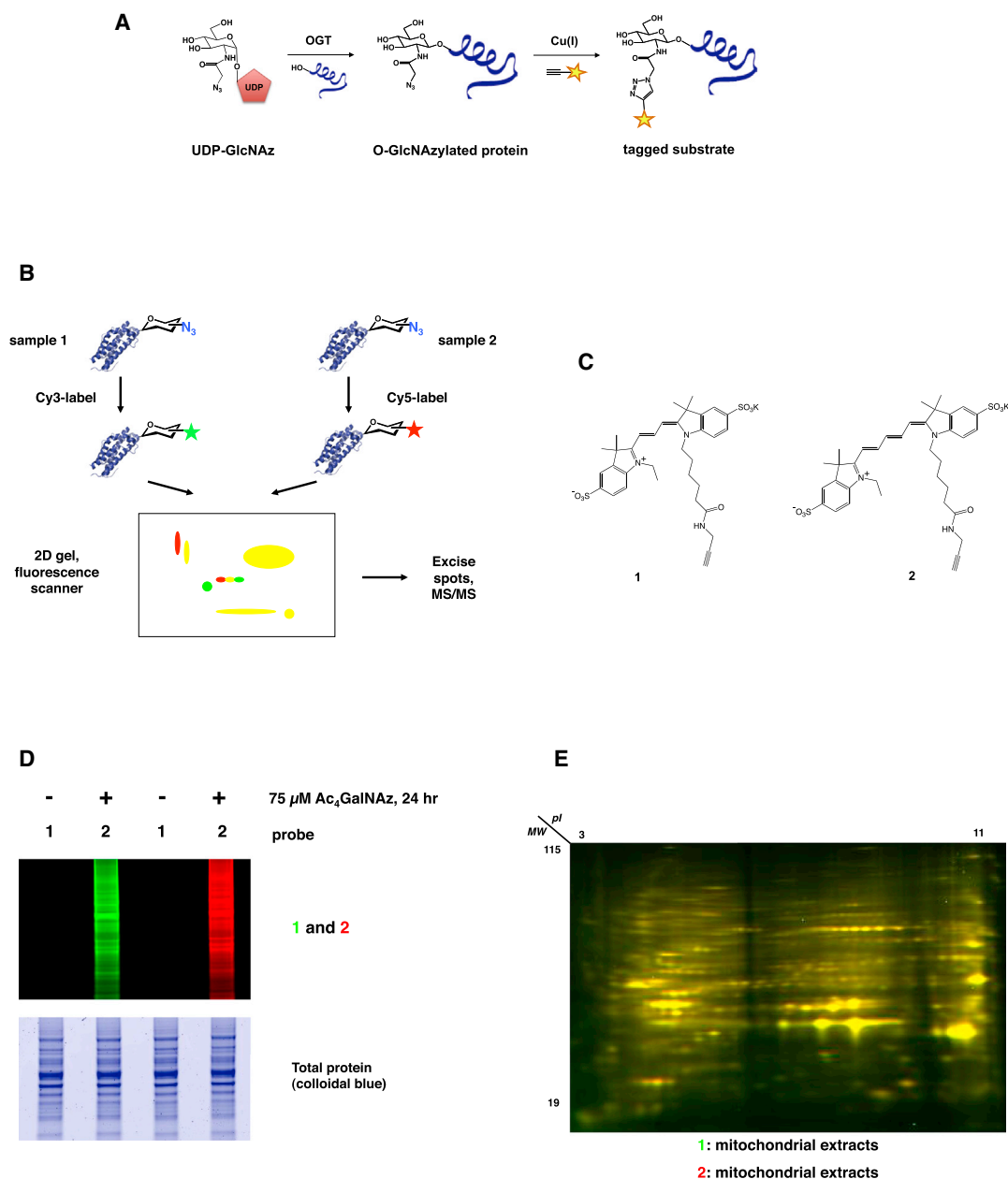
Figure 1. Glyco-DIGE System

(A) Endogenous O-GlcNAcylated proteins can be metabolically labeled by the conversion of GalNAz to UDP-GlcNAz, as described (Boyce et al., 2011). Such O-GlcNAzylated substrates can then be detected by chemical tagging with one of several azide-reactive probes. CuAAC is depicted here. The yellow stars represent a useful chemical moiety on the probe molecule, such as a fluorophore or affinity handle.

(B) Glyco-DIGE workflow is illustrated. First, protein extracts are made from two populations of cells (e.g., control and drug treated) that have been treated with GalNAz to metabolically label O-GlcNAc substrates with an azidoglycan (O-GlcNAz), as described (Boyce et al., 2011). The two protein samples are then labeled separately with azide-reactive Cy3- and Cy5-based dyes, mixed, and analyzed by 2D gel (horizontal dimension is for IEF; vertical dimension is for SDS-PAGE). When the gel is scanned, protein spots unchanged between samples appear as dual-color overlap (yellow), whereas proteins unique to one sample appear as single color spots (green indicates Cy3; red indicates Cy5), thereby permitting ready detection of sample-specific changes in O-GlcNAcylated proteins.

(C) Glyco-DIGE alkyne-functionalized fluorescent probes are shown.

(D) Glyco-DIGE probes specifically label azidosugar-tagged mammalian proteins. Jurkat cells were metabolically labeled with 100 μM peracetylated GalNAz (Ac$_4$GalNAz) or vehicle only for 24 hr. Whole-cell lysates were reacted with **1** or **2** via CuAAC and analyzed by standard SDS-PAGE and fluorescence scanning.

(E) **1** and **2** do not differentially affect protein migration in 2D gels. Jurkat cells were metabolically labeled with 100 μM Ac$_4$GalNAz for 24 hr. Then, mitochondria were purified and extracted into lysis buffer. Half the sample was labeled with **1** and half with **2**, and labeled samples were analyzed by glyco-DIGE. **1** is indicated in green, **2** in red, and **1**+**2** overlap in yellow.

See also Figure S8.

identifying compartment- or stimulus-specific changes in O-GlcNAcylated proteins across different samples, circumventing major, inherent disadvantages of affinity-based approaches. Furthermore, we use our approach to identify a mitochondrial glycoprotein and demonstrate its functional link to O-GlcNAc signaling.

RESULTS

Glyco-DIGE Permits Simultaneous Detection and Analysis of Hundreds of O-GlcNAcylated Proteins

To analyze sample-specific changes in O-GlcNAcylated proteins, we turned to difference gel electrophoresis (DIGE) (Minden et al., 2009). In traditional DIGE experiments, each of two protein samples (e.g., from control versus stimulated cells) is covalently labeled with a protein-nonspecific, cyanine 3 (Cy3)- or cyanine 5 (Cy5)-based fluorophore (Minden et al., 2009). Then, the samples are mixed and analyzed by conventional 2D electrophoresis (isoelectric focusing [IEF] followed by SDS-PAGE). When these 2D gels are imaged for Cy3 and Cy5, proteins that are unchanged between the two samples show perfect overlap of Cy3 and Cy5 fluorescence, whereas the rare proteins that are different between the two samples are visualized as Cy3-only or Cy5-only signal. These sample-specific proteins of interest can be excised from the gel and identified by mass spectrometry.

We envisioned that DIGE methods could be adapted to analyze glycoproteins, including O-GlcNAcylated substrates tagged via our GalNAz label and appropriate azide-reactive Cy3 and Cy5 derivatives, permitting us to visualize and identify sample-specific changes in O-GlcNAcylated proteins (Figures 1A and 1B). Furthermore, we hypothesized that this "glyco-DIGE" platform would permit the visualization of rare, sample-dependent changes in O-GlcNAcylated proteins, even in experiments where abundant, unchanging background O-GlcNAc is present elsewhere on the same 2D gel. Importantly, such a glyco-DIGE approach could detect any alteration in an O-GlcNAcylated protein that affected its mobility on a 2D gel, including de novo (de)glycosylation and other changes (e.g., cleavage, ubiquitination), providing broad information on the role of O-GlcNAcylated proteins in dynamic cell signaling.

To test the utility of a glyco-DIGE approach, we synthesized alkyne-functionalized Cy3 (**1**) and Cy5 (**2**) (Figure 1C). As expected, **1** and **2** reacted specifically with O-GlcNAcylated proteins from Jurkat cells metabolically labeled with GalNAz via the well-characterized, bioorthogonal copper-catalyzed azide-alkyne cycloaddition (CuAAC) reaction (Nwe and Brechbiel, 2009) (Figure 1D). Importantly, whereas hundreds of **1**- and **2**-labeled protein spots could be separated and visualized efficiently on the same glyco-DIGE gel, labeling by **1** or **2** did not differentially affect the migration of proteins in a glyco-DIGE experiment (Figure 1E). We concluded that glyco-DIGE can label and compare large numbers of O-GlcNAcylated proteins across different mammalian samples.

Glyco-DIGE Identifies VDAC2 as a Mitochondrial O-GlcNAc Substrate

We next asked whether glyco-DIGE could detect sample-specific differences in O-GlcNAcylated proteins. As a proof of principle experiment, we examined differences in protein glycosylation between mitochondria and cytosol. Although O-GlcNAc is a well-known sentinel of cellular glucose levels (Hanover et al., 2010; Hart et al., 2011) and regulates both metabolic (Dentin et al., 2008; Yang et al., 2008) and mitochondrial (Hu et al., 2009; Wang and Schwarz, 2009) pathways, the mitochondrial glycoproteome has not been analyzed systematically. We used glyco-DIGE to compare O-GlcNAcylated proteins from mitochondrial and cytosolic extracts (Figure S1) (Frezza et al., 2007) of the same human cell line. As expected, we detected numerous differences in the respective glycoproteomes of these two compartments (Figure 2A). Across many experiments and multiple cell types, we noticed one set of especially prominent mitochondrial O-GlcNAcylated protein spots (Figure 2A, arrows). Using fluorescence as a guide, we excised the corresponding spots from preparative gels and identified the voltage-dependent anion channel 2 (VDAC2) protein as the major component (Figure S2).
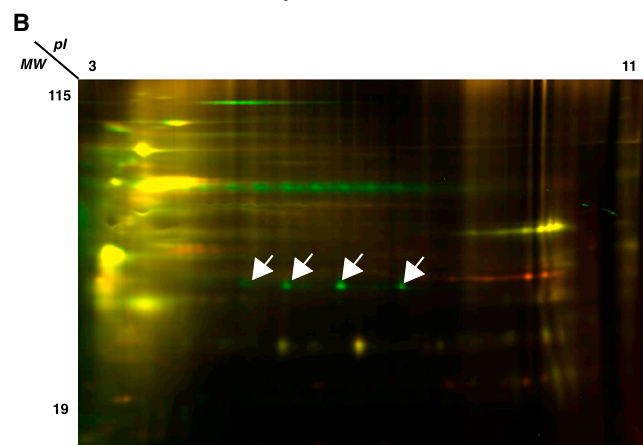
VDAC2 is a member of a family of multipass channel proteins residing in the mitochondrial outer membrane, with important roles in organelle metabolite flux, nutrient metabolism, and apoptotic signaling (Cheng et al., 2003; Ren et al., 2009; Shoshan-Barmatz et al., 2010). Although some work has suggested that VDAC family proteins might be glycosylated (Jones et al., 2008), VDAC2 had not been described or validated as a specific O-GlcNAc substrate. We performed two experiments to confirm our glyco-DIGE results with VDAC2. First, we compared mitochondrial extracts from wild-type and $VDAC2^{-/-}$ mouse embryonic fibroblasts (MEFs) (Cheng et al., 2003) in a glyco-DIGE experiment (Figure 2B). As expected, we found that spots corresponding to the ones identified in human cells were present in wild-type MEF mitochondrial samples but absent from the $VDAC2^{-/-}$ samples, indicating that these spots are VDAC2 (Figure 2B). Furthermore, these fluorescent spots correlated with anti-VDAC2 immunoreactivity on a 2D immunoblot of wild-type mitochondrial extracts (Figure S3). Second, we used an affinity approach (Boyce et al., 2011) to confirm our glyco-DIGE results with VDAC2. We labeled wild-type or $VDAC2^{-/-}$ MEFs with GalNAz, made mitochondrial extracts, and reacted them with phosphine-biotin to tag azide-bearing proteins. Then, we enriched for GalNAz-labeled proteins via anti-biotin affinity chromatography. As expected, anti-VDAC2 immunoblotting showed that VDAC2 was affinity purified only from wild-type mitochondrial samples from cells labeled with GalNAz (Figure 2C), demonstrating the specificity of GalNAz labeling of VDAC2. As further confirmation, we analyzed similar biotin affinity-purified samples by mass spectrometry and detected enrichment of VDAC2 in mitochondrial extracts from GalNAz-treated, but not vehicle-treated, wild-type MEFs (Figure S4). Taken together, these results indicate that VDAC2 is an O-GlcNAcylated mitochondrial protein in human and mouse cells.

Loss of VDAC2 Protects Cells from Mitochondrial Dysfunction and Apoptosis following Global Perturbation of O-GlcNAcylation

Intriguingly, VDAC2 (Cheng et al., 2003; Ren et al., 2009; Shoshan-Barmatz et al., 2010) and O-GlcNAc (Hu et al., 2009; Wang and Schwarz, 2009) are both critical regulators of

A

pl
MW   3   11
115

19
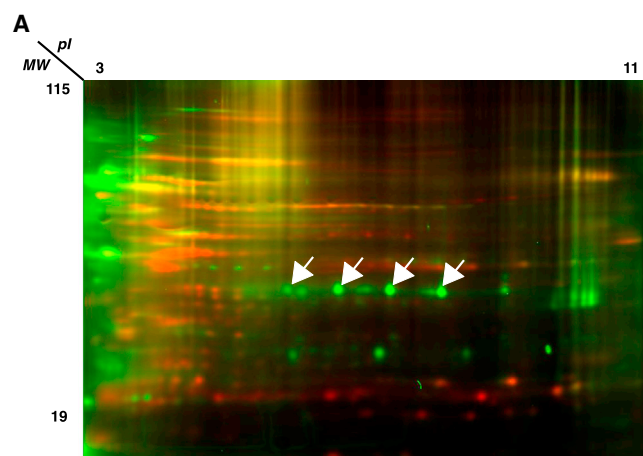
1: mitochondrial extracts

2: cytosolic extracts

B

pl
MW   3   11
115

19

1: wild type mitochondrial extracts

2: VDAC2⁻/⁻ mitochondrial extracts

C

α-biotin pulldown   input (3%)

WT Ø WT Ø   WT Ø WT Ø   genotype
−   −   +   +   −   −   +   +   Ac₄GalNAz (100 μM)
+   +   +   +   +   +   +   +   phosphine-biotin reaction
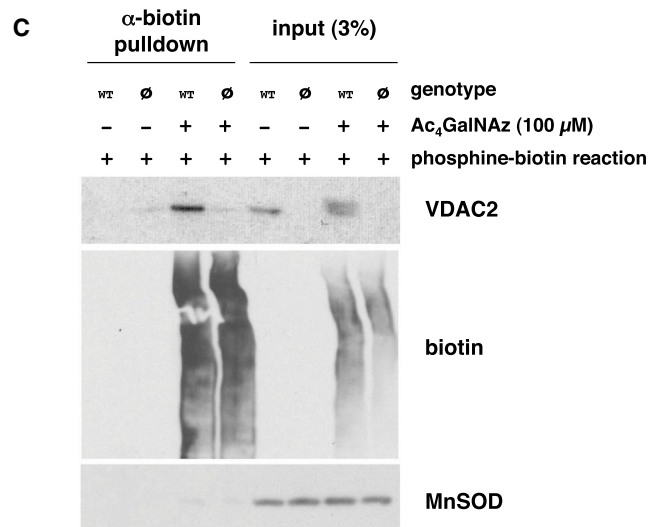
VDAC2

biotin

MnSOD

Figure 2. Glyco-DIGE Identifies VDAC2 as a Mitochondrial Glyco-protein

(A) Jurkat cells were metabolically labeled with 100 μM Ac₄GalNAz for 24 hr, and mitochondrial and cytosolic extracts were prepared. Mitochondrial extracts were reacted with **1** (green), and cytosolic extracts with **2** (red). Then, the samples were mixed and analyzed by glyco-DIGE. **1**+**2** overlap is indicated in yellow. Arrows point to VDAC2 spots. The characteristic "charge train" pattern of VDAC2 spots likely reflects the presence of multiple phosphorylated forms of the protein.

(B) Wild-type and $VDAC2^{-/-}$ MEFs were metabolically labeled with 100 μM Ac₄GalNAz for 24 hr. Mitochondrial extracts were prepared and labeled with 1 (wild-type is in green) or 2 ($VDAC2^{-/-}$ is in red) and then analyzed by glyco-DIGE. Arrows indicate VDAC2 spots.

(C) Wild-type (WT) and $VDAC2^{-/-}$ (ø) MEFs were metabolically labeled with 100 μM Ac₄GalNAz or vehicle only for 24 hr, and mitochondrial extracts were prepared and reacted with phosphine-biotin. Then, biotin-tagged proteins were affinity purified essentially as described (Boyce et al., 2011) and analyzed by immunoblot. Left view shows affinity-purified material. Right view presents 3% total input of material (loading control). MnSOD serves as a loading control for total mitochondrial protein and demonstrates the removal of un-glycosylated proteins during affinity purification.

See also Figures S1, S2, S3, and S4.

mitochondrial metabolism and cell death, but no experimental evidence had established a functional connection between them. Given our finding that VDAC2 is a glycoprotein, we asked whether a phenotypic relationship existed between O-GlcNAc signaling and VDAC2. We found that potentiating global O-GlcNAc levels using a combination of glucosamine, to increase levels of UDP-GlcNAc (Vosseller et al., 2002), and Thiamet-G, a specific small molecule inhibitor of the glycoside hydrolase O-GlcNAcase (OGA) (Yuzwa et al., 2008), resulted in mitochondrial dysfunction and apoptosis in MEFs (Figure 3). Consistent with previous reports by Gloster et al. (2011) and Slawson et al. (2005), both wild-type and $VDAC2^{-/-}$ MEFs altered OGA and OGT protein levels to compensate for the pharmacological perturbation of O-GlcNAc, especially at later time points (Figures 3B and S5). Nevertheless, we found that $VDAC2^{-/-}$ MEFs were resistant to the mitochondrial dysfunction (Figure 3A) and apoptosis (Figure 3B) caused by Thiamet-G and glucosamine. Furthermore, this difference was caused by the loss of VDAC2 per se, and not an adventitious or irreversible downstream effect of gene deletion, because stable re-expression of VDAC2 in $VDAC2^{-/-}$ MEFs restored sensitivity to Thiamet-G/glucosamine treatment (Figure S6). We concluded that global O-GlcNAc perturbation induces mitochondrial dysfunction and apoptosis and that VDAC2 is required for these effects, demonstrating a critical functional connection between VDAC2 and O-GlcNAc signaling in organelle physiology and cell death.

DISCUSSION

We have developed a proteomics platform, termed glyco-DIGE, which can detect differences in O-GlcNAcylated proteins across samples. Importantly, the combination of GalNAz labeling and glyco-DIGE permits time-resolved examination of new cellular O-GlcNAc and allows the detection of rare, substoichiometric, sample-dependent changes in O-GlcNAcylated substrates, without incurring the bias toward abundant, unchanging, multiply glycosylated "background" substrates that is endemic to affinity-based analysis of O-GlcNAc. Therefore, whereas
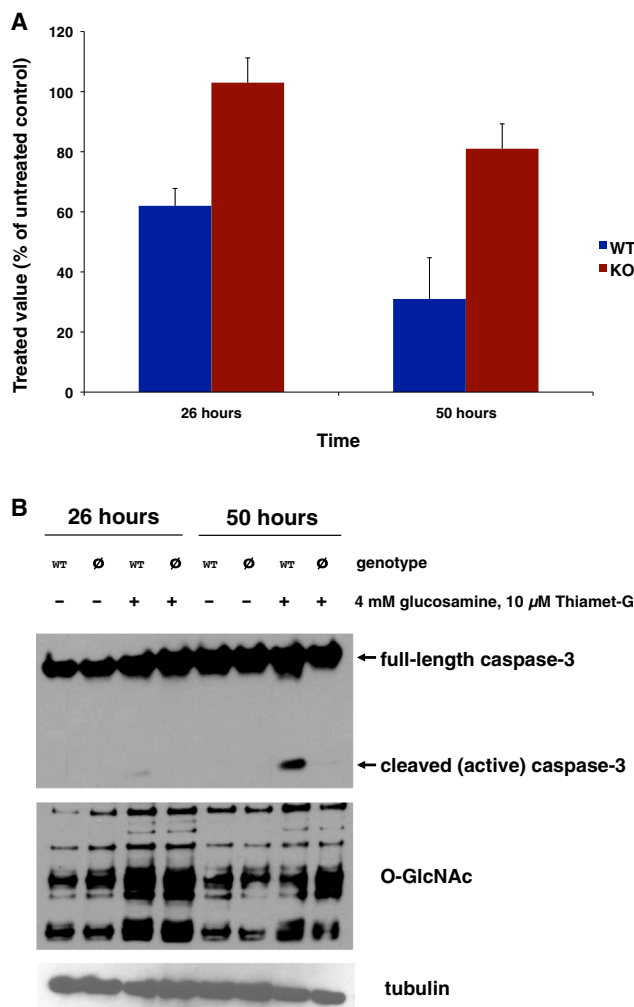
Figure 3. Loss of VDAC2 Protects Cells from Mitochondrial Dysfunction and Cell Death Induced by Global O-GlcNAc Perturbation

(A) Wild-type or $VDAC2^{-/-}$ cells were treated with 10 μM Thiamet-G and 4 mM glucosamine or vehicle control for 26 or 50 hr and analyzed by MTS assay to measure mitochondrially produced reducing equivalents (i.e., NADH and NADPH). Treated samples were normalized to their corresponding vehicle-only controls. Error bars represent SDs.

(B) Wild-type or $VDAC2^{-/-}$ cells were treated as in (A), and whole-cell lysates were prepared and analyzed by immunoblot as indicated.

See also Figures S5 and S6.

affinity-based approaches will remain valuable for the bulk identification of O-GlcNAc substrates, we anticipate that GalNAz labeling and glyco-DIGE will provide an important complementary method to examine subtle, functionally relevant changes in O-GlcNAc. In a proof-of-principle experiment, we used glyco-DIGE to perform an unbiased search for mitochondria-specific O-GlcNAcylated proteins (Figure 2). We expect that our method will also lend itself to numerous applications for examining signal-dependent changes in O-GlcNAc. For example, in preliminary experiments, we used glyco-DIGE to examine differences in nuclear O-GlcNAcylated proteins in control versus DNA-

damaged cells and found genotoxic stress-specific changes conserved across disparate human cell lines (Figure S7). The identification of these and other signal-specific glyco-DIGE protein spots is ongoing. More generally, we note that conventional DIGE methods can resolve ~2,500 cyanine-labeled protein spots from samples of 1,000–10,000 mammalian cells (Meyer and Stühler, 2007; Minden et al., 2009), and we anticipate that glyco-DIGE capabilities will be comparable. In addition, glyco-DIGE experiments can be easily tailored to specific pI and molecular weight (MW) ranges (narrow or broad, as appropriate) using commercial reagents, and glyco-DIGE is compatible with a wide variety of biochemical procedures for sample prefractionation. Therefore, glyco-DIGE will be useful in analyzing even more complex biological samples in the future.

In the current work, we used glyco-DIGE to identify VDAC2 as a mitochondrial O-GlcNAc substrate and showed that the mitochondrial dysfunction and cell death caused by global O-GlcNAc perturbation depend on VDAC2. Interestingly, although VDAC2 has a previously described role in apoptosis, its loss was shown to sensitize cells to such stimuli as protein kinase inhibition, genotoxic stress (Cheng et al., 2003), and T cell receptor ligation (Ren et al., 2009), whereas we find that the loss of VDAC2 protects cells from global O-GlcNAc perturbation. Given the well-known roles of O-GlcNAc and VDAC2 in apoptotic signaling and cell metabolism, it will be interesting to dissect the molecular explanation for VDAC2's various pro- and antiapoptotic effects in response to distinct stimuli and determine whether these phenotypes are controlled directly by O-GlcNAcylation of VDAC2 itself and/or by other mechanisms. To this end, we are working to identify the glycosylation site(s) on VDAC2 and will use unglycosylatable mutants to address these questions in future work. Beyond mitochondrial O-GlcNAc, we believe glyco-DIGE will serve as a useful tool for analyzing rare, signal-dependent changes in O-GlcNAcylated proteins, providing a powerful complement to existing affinity-based approaches for studying O-GlcNAc signaling in a wide range of experimental contexts.

EXPERIMENTAL PROCEDURES

Compound Synthesis and Small Molecule Reagents

Glyco-DIGE probes **1** and **2** were synthesized from propargyl amine and *N*-hydroxysuccinamide esters of Cy3 and Cy5, respectively (GE Healthcare), and purified by reversed-phase high-performance liquid chromatography. See Extended Experimental Procedures for details. Syntheses and purification of peracetylated GalNAz (Laughlin and Bertozzi, 2007), phosphine-biotin (Saxon and Bertozzi, 2000), and Thiamet-G (Yuzwa et al., 2008) were performed essentially as described. Other chemical reagents were obtained from Sigma-Aldrich unless otherwise indicated.

Cell Culture, Treatment, and Protein Sample Preparation

Cells were maintained in a 5% CO_2, humidified atmosphere at 37°C in medium (Jurkat: RPMI 1640; MEFs, HT1080, 293T: Dulbecco's modified Eagle's medium) plus 10% fetal bovine serum and penicillin/streptomycin (Invitrogen). A total of 100 mM DMSO stock solution of peracetylated GalNAz was added to achieve final treatment conditions.

For whole-cell lysates, cells were treated as indicated, washed in cold PBS, and resuspended in Buffer L (1% Triton X-100, 150 mM NaCl, 20 mM Tris-HCl [pH 7.4]) plus Protease Inhibitor Cocktail III (Calbiochem). Lysates were probe sonicated (Misonix) on ice for 1 min and cleared by centrifugation.

For subcellular fractionation, mitochondria were prepared as described by Frezza et al. (2007), and mitochondrial protein extracts were made from

purified organelles as outlined above. For cytosolic protein extracts, supernatant from the final spin of the mitochondrial preparation was cleared by high-speed centrifugation and brought to Buffer L reagent concentrations. Highly purified nuclear extracts were prepared as described (Boyce et al., 2011). Where indicated (Figure S1), nuclear/cytoplasmic fractions were prepared by recombining the nuclear and cytoplasmic material after isolation of mitochondria. The quality of subcellular fractionations was verified by immunoblot for known organelle marker proteins (Figures 2C and S1).

For DNA damage experiments, cells were treated with 100 μM GalNAz and either 1 μg/ml doxorubicin or vehicle control (DMSO) for 24 hr. Then, nuclear extracts were made and analyzed pairwise (i.e., with versus without doxorubicin) in glyco-DIGE experiments as described below.

In all cases, protein concentrations were quantified by bicinchoninic acid assay (Thermo Fisher Scientific), and all samples were normalized with buffer to the same total protein concentration. Where indicated, equal protein loading was verified by control immunoblot (e.g., tubulin, MnSOD) or colloidal blue stain (Invitrogen).

Bioorthogonal Reactions of Azides

For CuAAC reactions, protein extracts were mixed with 25 μM **1** or **2** as indicated, 5 mM sodium ascorbate, 100 μM Tris[(1-benzyl-1H-1,2,3-triazol-4-yl)methyl]amine (TBTA), and 1 mM CuSO$_4$ (final concentrations) from the following stock solutions: 10 mM **1** or **2** (in water); 167 mM sodium ascorbate (in water, prepared fresh); 30 mM TBTA (in DMSO); and 50 mM CuSO$_4$ (in water). Reactions were incubated in the dark with end-over-end inversion for 1 hr and then stopped by addition of 10 mM (final) EDTA.

For Staudinger ligation reactions, protein extracts were mixed with 500 μM phosphine-biotin (final concentration, from 5 mM stock in 30% dimethylformamide in PBS) and incubated overnight with end-over-end inversion. NeutrAvidin antibiotin affinity chromatography was performed as described (Boyce et al., 2011).

Glyco-DIGE Sample Analysis and Spot Picking

To perform a glyco-DIGE experiment, equal protein amounts of **1**- and **2**-labeled samples were combined, and excess, unreacted alkyne probe was removed by exchange into Buffer L plus 10 mM EDTA using Bio-Spin P-6 columns (Bio-Rad). Labeled protein was precipitated and washed using the 2D Clean-Up Kit (GE Healthcare) and dissolved in DeStreak Rehydration Solution (GE Healthcare) with 20 mM dithiothreitol (DTT) and 0.5% IPG Buffer pH 3–10 NL (GE Healthcare).

For the IEF dimension, samples (200 μg to 1 mg of protein) were rehydration loaded onto 11 cm pH 3–11 NL Immobiline DryStrip IEF strips (GE Healthcare) using an Ettan IPGphor 3 IEF unit according to the manufacturer's instructions. For the second (i.e., SDS-PAGE) dimension, IEF strips were equilibrated by incubation in SDS equilibration buffer (6 M urea, 75 mM Tris-HCl [pH 8.8], 29.3% glycerol, 2% SDS, bromophenol blue) with 10 mg/ml DTT for 15 min, followed by incubation in SDS equilibration buffer with 25 mg/ml iodoacetamide for 15 min. Equilibrated strips were laid over precast 10% or 4%–20% gradient Criterion IEF SDS-PAGE gels (Bio-Rad) and sealed into place using 1% agarose and bromophenol blue in 1× MES buffer (Bio-Rad). Standard SDS-PAGE was then performed using the Criterion gel system (Bio-Rad).

Finished glyco-DIGE gels were washed briefly in ultrapure water and immobilized by sealing with 1% agarose in water onto a custom-built low-fluorescence glass stage marked with fluorescent stickers (GE Healthcare). Immobilized gels were scanned on a Typhoon flatbed gel scanner (GE Healthcare) using the factory preset excitation and emission settings for Cy3 and Cy5 and DIGE data acquisition mode. Data were analyzed using ImageQuant TL software (GE Healthcare). Fluorescent protein spots of interest were identified by inspection and marked via the ImageQuant 2D gel analysis tool to make a pick list, using the fluorescent guide stickers as reference coordinates. Gel coordinates of spots on the pick list were exported to Excel (Microsoft) and converted to a text file using an in-house macro. Spots from the pick list were excised from the gel using an Ettan Spot Picker robot (GE Healthcare) according to the manufacturer's instructions into 96-well plates. Gel picks from the same spot were pooled by hand for proteomic analysis.

Immunoblotting

Immunoblotting was performed essentially as described (Boyce et al., 2011). See Extended Experimental Procedures for details.

Mass Spectrometric Analysis

Samples were subjected to reversed-phase chromatography with an Agilent 1200 liquid chromatography system connected in-line to either an LTQ XL mass spectrometer or an LTQ Orbitrap XL hybrid mass spectrometer and processed using customized data-dependent acquisition methods. Protein identities were obtained using the SEQUEST search algorithm within Proteome Discoverer 1.3 (Thermo Fisher Scientific). See Extended Experimental Procedures for details.

Assay of Mitochondrial Function

Wild-type and $VDAC2^{-/-}$ MEFs were plated in 96-well plates (5,000 cells/well) in phenol red-free medium (Invitrogen). Cells were treated as indicated and analyzed by CellTiter AQueous One Solution Cell Proliferation Assay (to measure reducing equivalents, NADH and NADPH) or Caspase-Glo 3/7 Assay (to measure apoptotic protease activity) (Promega) according to the manufacturer's instructions. Results were read using a Molecular Devices SpectraMax automated plate reader using the appropriate factory preset parameters.

SUPPLEMENTAL INFORMATION

Supplemental Information includes Extended Experimental Procedures and eight figures and can be found with this article online at http://dx.doi.org/10.1016/j.celrep.2013.08.048.

REFERENCES

Boyce, M., and Bertozzi, C.R. (2011). Bringing chemistry to life. Nat. Methods *8*, 638–642.

Boyce, M., Carrico, I.S., Ganguli, A.S., Yu, S.H., Hangauer, M.J., Hubbard, S.C., Kohler, J.J., and Bertozzi, C.R. (2011). Metabolic cross-talk allows labeling of O-linked beta-N-acetylglucosamine-modified proteins via the N-acetylgalactosamine salvage pathway. Proc. Natl. Acad. Sci. USA *108*, 3141–3146.

Cheng, E.H., Sheiko, T.V., Fisher, J.K., Craigen, W.J., and Korsmeyer, S.J. (2003). VDAC2 inhibits BAK activation and mitochondrial apoptosis. Science *301*, 513–517.

Dentin, R., Hedrick, S., Xie, J., Yates, J., 3rd, and Montminy, M. (2008). Hepatic glucose sensing via the CREB coactivator CRTC2. Science *319*, 1402–1405.

Frezza, C., Cipolat, S., and Scorrano, L. (2007). Organelle isolation: functional mitochondria from mouse liver, muscle and cultured fibroblasts. Nat. Protoc. *2*, 287–295.

Gloster, T.M., Zandberg, W.F., Heinonen, J.E., Shen, D.L., Deng, L., and Vocadlo, D.J. (2011). Hijacking a biosynthetic pathway yields a glycosyltransferase inhibitor within cells. Nat. Chem. Biol. *7*, 174–181.

Hanover, J.A., Krause, M.W., and Love, D.C. (2010). The hexosamine signaling pathway: O-GlcNAc cycling in feast or famine. Biochim. Biophys. Acta *1800*, 80–95.

Hart, G.W., Slawson, C., Ramirez-Correa, G., and Lagerlof, O. (2011). Cross talk between O-GlcNAcylation and phosphorylation: roles in signaling, transcription, and chronic disease. Annu. Rev. Biochem. 80, 825–858.

Hu, Y., Suarez, J., Fricovsky, E., Wang, H., Scott, B.T., Trauger, S.A., Han, W., Hu, Y., Oyeleye, M.O., and Dillmann, W.H. (2009). Increased enzymatic O-GlcNAcylation of mitochondrial proteins impairs mitochondrial function in cardiac myocytes exposed to high glucose. J. Biol. Chem. 284, 547–555.

Jones, S.P., Zachara, N.E., Ngoh, G.A., Hill, B.G., Teshima, Y., Bhatnagar, A., Hart, G.W., and Marbán, E. (2008). Cardioprotection by N-acetylglucosamine linkage to cellular proteins. Circulation 117, 1172–1182.

Khidekel, N., Arndt, S., Lamarre-Vincent, N., Lippert, A., Poulin-Kerstien, K.G., Ramakrishnan, B., Qasba, P.K., and Hsieh-Wilson, L.C. (2003). A chemoenzymatic approach toward the rapid and sensitive detection of O-GlcNAc posttranslational modifications. J. Am. Chem. Soc. 125, 16162–16163.

Laughlin, S.T., and Bertozzi, C.R. (2007). Metabolic labeling of glycans with azido sugars and subsequent glycan-profiling and visualization via Staudinger ligation. Nat. Protoc. 2, 2930–2944.

Meyer, H.E., and Stühler, K. (2007). High-performance proteomics as a tool in biomarker discovery. Proteomics 7(Suppl 1), 18–26.

Minden, J.S., Dowd, S.R., Meyer, H.E., and Stühler, K. (2009). Difference gel electrophoresis. Electrophoresis 30(Suppl 1), S156–S161.

Nwe, K., and Brechbiel, M.W. (2009). Growing applications of "click chemistry" for bioconjugation in contemporary biomedical research. Cancer Biother. Radiopharm. 24, 289–302.

Ren, D., Kim, H., Tu, H.C., Westergard, T.D., Fisher, J.K., Rubens, J.A., Korsmeyer, S.J., Hsieh, J.J., and Cheng, E.H. (2009). The VDAC2-BAK rheostat controls thymocyte survival. Sci. Signal. 2, ra48.

Saxon, E., and Bertozzi, C.R. (2000). Cell surface engineering by a modified Staudinger reaction. Science 287, 2007–2010.

Shoshan-Barmatz, V., De Pinto, V., Zweckstetter, M., Raviv, Z., Keinan, N., and Arbel, N. (2010). VDAC, a multi-functional mitochondrial protein regulating cell life and death. Mol. Aspects Med. 31, 227–285.

Slawson, C., Zachara, N.E., Vosseller, K., Cheung, W.D., Lane, M.D., and Hart, G.W. (2005). Perturbations in O-linked beta-N-acetylglucosamine protein modification cause severe defects in mitotic progression and cytokinesis. J. Biol. Chem. 280, 32944–32956.

Teo, C.F., Ingale, S., Wolfert, M.A., Elsayed, G.A., Nöt, L.G., Chatham, J.C., Wells, L., and Boons, G.J. (2010). Glycopeptide-specific monoclonal antibodies suggest new roles for O-GlcNAc. Nat. Chem. Biol. 6, 338–343.

Vocadlo, D.J., Hang, H.C., Kim, E.J., Hanover, J.A., and Bertozzi, C.R. (2003). A chemical approach for identifying O-GlcNAc-modified proteins in cells. Proc. Natl. Acad. Sci. USA 100, 9116–9121.

Vosseller, K., Wells, L., Lane, M.D., and Hart, G.W. (2002). Elevated nucleocytoplasmic glycosylation by O-GlcNAc results in insulin resistance associated with defects in Akt activation in 3T3-L1 adipocytes. Proc. Natl. Acad. Sci. USA 99, 5313–5318.

Vosseller, K., Trinidad, J.C., Chalkley, R.J., Specht, C.G., Thalhammer, A., Lynn, A.J., Snedecor, J.O., Guan, S., Medzihradszky, K.F., Maltby, D.A., et al. (2006). O-linked N-acetylglucosamine proteomics of postsynaptic density preparations using lectin weak affinity chromatography and mass spectrometry. Mol. Cell. Proteomics 5, 923–934.

Wang, X., and Schwarz, T.L. (2009). The mechanism of Ca2+ -dependent regulation of kinesin-mediated mitochondrial motility. Cell 136, 163–174.

Wells, L., Vosseller, K., Cole, R.N., Cronshaw, J.M., Matunis, M.J., and Hart, G.W. (2002). Mapping sites of O-GlcNAc modification using affinity tags for serine and threonine post-translational modifications. Mol. Cell. Proteomics 1, 791–804.

Yang, X., Ongusaha, P.P., Miles, P.D., Havstad, J.C., Zhang, F., So, W.V., Kudlow, J.E., Michell, R.H., Olefsky, J.M., Field, S.J., and Evans, R.M. (2008). Phosphoinositide signalling links O-GlcNAc transferase to insulin resistance. Nature 451, 964–969.

Yuzwa, S.A., Macauley, M.S., Heinonen, J.E., Shan, X., Dennis, R.J., He, Y., Whitworth, G.E., Stubbs, K.A., McEachern, E.J., Davies, G.J., and Vocadlo, D.J. (2008). A potent mechanism-inspired O-GlcNAcase inhibitor that blocks phosphorylation of tau in vivo. Nat. Chem. Biol. 4, 483–490.